

## Quantized Vortices and Four-Component Superfluidity of Semiconductor Excitons

Romain Anankine,<sup>1</sup> Mussie Beian,<sup>1,2</sup> Suzanne Dang,<sup>1</sup> Mathieu Alloing,<sup>1</sup> Edmond Cambri,<sup>3</sup> Kamel Merghem,<sup>3</sup> Carmen Gomez Carbonell,<sup>3</sup> Aristide Lemaître,<sup>3</sup> and François Dubin<sup>1,\*</sup>

<sup>1</sup>*Sorbonne Universités, UPMC Univ. Paris 06, CNRS-UMR 7588, Institut des NanoSciences de Paris, 4 Place Jussieu, F-75005 Paris, France*

<sup>2</sup>*ICFO-The Institute of Photonic Sciences, Av. Carl Friedrich Gauss, num. 3, 08860 Castelldefels, Spain*

<sup>3</sup>*Laboratoire de Photonique et Nanostructures, LPN/CNRS, Route de Nozay, 91460 Marcoussis, France*  
(Received 26 July 2016; published 23 March 2017; publisher error corrected 24 March 2017)

We study spatially indirect excitons of GaAs quantum wells, confined in a 10  $\mu\text{m}$  electrostatic trap. Below a critical temperature of about 1 K, we detect macroscopic spatial coherence and quantized vortices in the weak photoluminescence emitted from the trap. These quantum signatures are restricted to a narrow range of density, in a dilute regime. They manifest the formation of a four-component superfluid, made by a low population of optically bright excitons coherently coupled to a dominant fraction of optically dark excitons.

DOI: 10.1103/PhysRevLett.118.127402

Massive bosonic particles realize a rich variety of collective quantum phenomena where their underlying fermionic structure is nevertheless hardly observed [1,2]. For example, Bose-Einstein condensation of atomic gases is generally understood by neglecting the atoms fermionic nature. Semiconductor excitons, i.e., Coulomb-bound electron-hole pairs, constitute a class of composite bosons which contrasts with this behavior. Indeed, Combescot and co-workers have predicted that the fermionic structure of excitons leads to a multicomponent condensate, with optically active and inactive parts that are coherently coupled through electron and/or hole exchanges between excitons [3–5].

Widely studied GaAs quantum wells provide an interesting playground to demonstrate the predictions made by Combescot and co-workers, and then possibly conclude a fifty-year long quest for Bose-Einstein condensation of excitons [6–9]. Indeed, in GaAs quantum wells lowest energy excitonic states exhibit a total “spin” ( $\pm 1$ ) or ( $\pm 2$ ). These states are then optically active and inactive, respectively, dark states lying at the lowest energy. Neglecting exciton-exciton interactions, Bose-Einstein condensation then leads to a macroscopic occupation of dark states so that the condensate is completely inactive optically [3]. Beyond a critical density, however, exciton-exciton interactions can dress the many-body ground state. Fermion exchanges then become crucial because they can coherently convert opposite spin dark excitons into opposite spin bright ones [10]. Thus, a small bright component is possibly introduced coherently into the dark condensate [4,5]. This results in a four-component many-body phase, which is gray, i.e., poorly active optically but possibly signaled by its weak photoluminescence coherent with the hidden dark part.

The dominantly dark nature of excitonic condensation manifests directly a high-temperature quantum phase transition. Indeed, in wide GaAs quantum wells the energy

splitting between bright and dark states is of the order of  $\mu\text{eV}$  [11], i.e., small compared to the thermal energy ( $\sim 2k_B$ ) at the condensation threshold [12]. As a result, a macroscopic population of dark excitons violates classical expectations. This point of view has long been overlooked by research of a condensate of bright excitons [8,13–15], until recent works have instead pointed out experimentally the role played by dark states below a few Kelvin. These studies were realized with long-lived spatially indirect excitons [16,17], engineered by enforcing a spatial separation between electrons and holes, for instance, by confining them in two adjacent GaAs quantum wells. Thus, a darkening of the photoluminescence has been reported below a few Kelvin [18]. Macroscopic spatial coherence of an anomalously dark gas has also been observed at sub-Kelvin temperatures [19].

Very recently, we have reported an important step towards unambiguous signatures for the dark state condensation of GaAs excitons [20]. Precisely, we have shown that indirect excitons can be confined in a 10  $\mu\text{m}$  electrostatic trap and studied at controlled densities and temperatures, in a regime of vanishingly small inhomogeneous broadening. This degree of control, never achieved before to the best of our knowledge, is necessary to evaluate the occupation of bright and dark states free from experimental uncertainties. Thus, we have shown unambiguously that the photoluminescence emission quenches below a critical temperature of about 1 K, when  $\sim 10^4$  indirect excitons are trapped [20]. The quenching was interpreted as the manifestation for the dark state condensation; however, the exact nature of the quantum phase remained inaccessible to these experiments relying on photoluminescence spectroscopy.

In this Letter, we report time and spatially resolved interferometry of the photoluminescence emitted by indirect excitons confined in a 10  $\mu\text{m}$  trap, down to the regime of photoluminescence quenching. Below a critical

temperature of about 1 K, we demonstrate macroscopic spatial coherence and quantized vortices restricted to a small range of excitonic density, precisely in a dilute regime when  $10^4 - 2 \times 10^4$  excitons are confined in the trap. These superfluid signatures emerge for a population of bright excitons about 3 times smaller than the one of dark excitons. Our findings thus evidence quantitatively the theoretically predicted gray condensation of indirect excitons [4]. This shows that bilayer GaAs heterostructures, either studied by photoluminescence [23–28] or transport techniques [29–32], open a versatile platform to develop quantum control in semiconductors.

As illustrated in Fig. 1(a), our experiments rely on a 100 ns long laser pulse that loads indirect excitons in a shallow electrostatic trap. The latter is realized by controlling the electric field in the plane of two 8 nm GaAs quantum wells, where photoinjected electrons and holes are

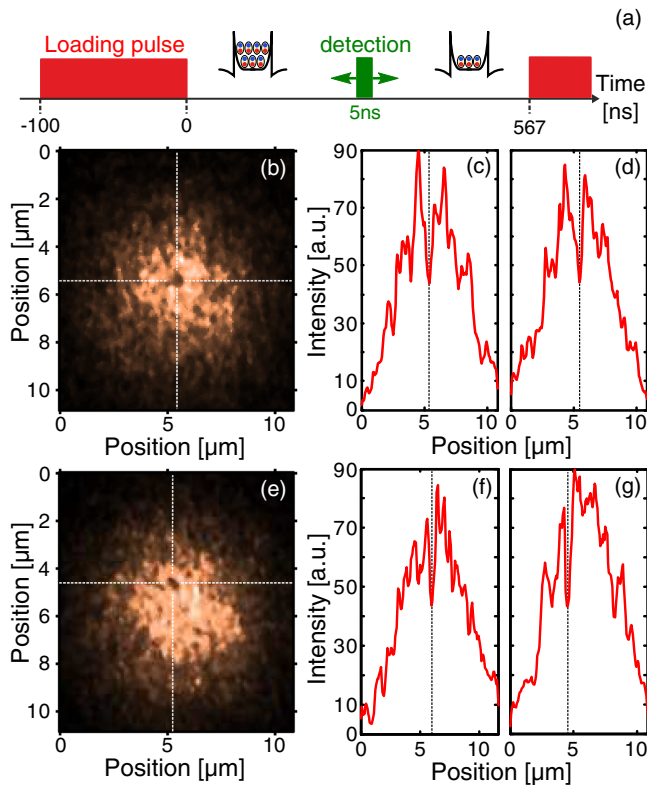


FIG. 1. (a) A 100 ns long loading laser pulse injects indirect excitons in a  $10 \mu\text{m}$  electrostatic trap. The reemitted photoluminescence is analyzed in a 5 ns long detection window, at a variable delay to the end of the loading pulse, the sequence being repeated at 1.5 MHz for 10–20 s typical acquisition times. (b)–(e) Photoluminescence emitted from the trap, at  $T_b = 330 \text{ mK}$ , and for a delay of 150 ns so that the number of trapped excitons is  $\sim 2 \times 10^4$ . Horizontal and vertical dashed lines highlight positions where we observe about 50% intensity loss along both the horizontal and vertical axis. This is shown by the profiles in (c)–(d) and (f)–(g) for the images shown in (b) and (e), respectively. Measurements have all been acquired successively for identical experimental settings, the acquisition time being 10 s.

confined (quantum wells being separated by a 4 nm AlGaAs barrier—see Supplemental Material [12] for more details). In the following, we emphasize the photoluminescence reemitted between 150 and 200 ns after extinction of the loading laser pulse. This delay range corresponds to about twice the indirect excitons optical lifetime [12]. During this time interval, the trapped gas is dilute and we estimate that the total number of excitons decreases from about  $2 \times 10^4$  to  $10^4$  [21,22]. Thus, we detect spectroscopically a highly nonclassical population of optically dark indirect excitons at sub-Kelvin bath temperatures [12,20]. At the same time, the photoluminescence emitted at the center of the trap is homogeneously broadened (see Fig. S1 of the Supplemental Material [12]).

In Fig. 1(b) we show the spatial profile of the photoluminescence emitted when  $\sim 2 \times 10^4$  excitons are trapped at a bath temperature  $T_b = 330 \text{ mK}$ . We strikingly note a very inhomogeneous intensity distribution, a dark spot being identified at the centre of the image, i.e., at the minimum of the trapping potential where the photoluminescence intensity is nevertheless the largest. At the center of the dark spot we observe a 50% loss of intensity [Figs. 1(c)–1(d)] corresponding to a twofold decrease of the population of bright excitons. This variation marks a deviation of  $\sim 5\sigma$  of the photoluminescence signal which is not interpretable in terms of intensity fluctuations.

In our experiments, the unambiguous detection of dark spots, as in Fig. 1(b), requires precise experimental settings. It is mostly achieved around the center of the trap, at sub-Kelvin bath temperatures and for less than about  $4 \times 10^4$  confined excitons, that is later than 120 ns after extinction of the loading pulse. Experimentally, a statistically unambiguous detection of dark spots resumes to a tradeoff between the signal to noise ratio and the number of individual realizations that we average, that is the acquisition time. The latter can not exceed about 10 s, because at  $T_b = 330 \text{ mK}$  dark spots emerge at uncorrelated positions during unchanged experimental settings. This behavior is signaled by comparing the emission profiles shown in Figs. 1(b) and 1(e). Both were recorded successively and in the same conditions, nevertheless they exhibit intensity losses localized at distinct positions in the central region of the trap.

We interpret the dark spots in the photoluminescence as a direct manifestation for the disorder of our electrostatic confinement. In Ref. [20] we have already highlighted that the trapping potential fluctuates during our experiments. The level of electrostatic disorder is such that it leads to stochastic variations of the photoluminescence spectral width, from  $\sim 300 \mu\text{eV}$  to  $\sim 1 \text{ meV}$  and within a time scale of a few seconds at  $T_b = 330 \text{ mK}$ . However, the electrostatic disorder can be turned into an advantage to signal quantum fingerprints for the regime of photoluminescence quenching [20]. Indeed, defects of the confining potential are energetically favorable positions to localize quantized

vortices and thus reveal a superfluid behavior. Vortices could then remain pinned in the trapping potential, the only situation to actually detect them by our experiments which rely on averaging  $\sim 10^7$  single-shot images during 10 s.

To assess whether dark spots detected at the center of the trap can manifest quantized vortices pinned by electrostatic disorder, we analyzed the spatial coherence of the photoluminescence with a Mach-Zehnder interferometer. The interferometer is stabilized with a vanishing path length difference between its two arms, one of which horizontally displaces its output by  $2\ \mu\text{m}$  compared to the other arm [19], i.e., by 10 times the thermal wavelength of excitons at our lowest bath temperature. Because of a vertical tilt angle deliberately introduced between the two arms, a condensate with complete long-range order leads to horizontally aligned interference fringes [Fig. 2(a)]. A vortex pinned around the center of such a condensate then appears through the inclusion of a “ring” in the central bright fringe, as shown in Fig. 2(b). This pattern is understood by noting that on each side of the ring the vortex and its shifted image interfere with  $2\ \mu\text{m}$  distant regions where the phase is well defined. Forklike dislocations are thus created at these two locations since the phase of the wave function winds by  $2\pi$  around the core of a vortex [1,2]. The superposition of the two mirrored and shifted forks leads

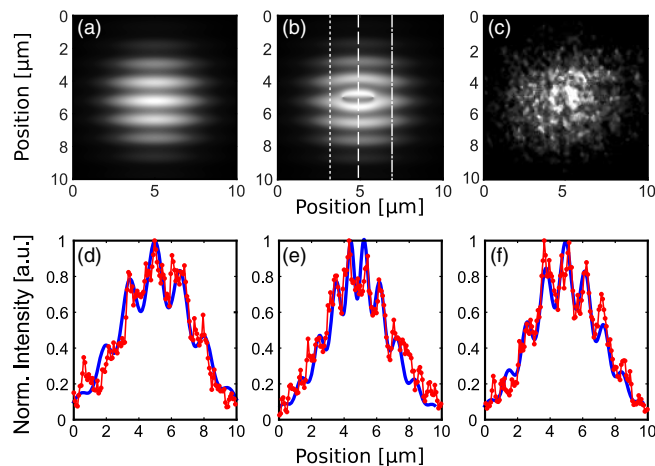


FIG. 2. Simulation of the interference pattern for a condensate with complete long-range order in the trap (a), and for a condensate constraining one quantized vortex at the center of the trap (b). Two phase singularities are observed in the latter case, on each side of a ring-shaped interference fringe. (c) Interference pattern measured when  $\sim 2 \times 10^4$  excitons are confined in the trap at  $T_b = 330$  mK. These experiments were realized in the same conditions as for the measurements shown in Fig. 1(b). (d)–(f) Red points show the interference profiles measured, as highlighted in (b), at the center of the ring (e), on its left (d) and right (f). The solid blue lines display the patterns simulated by modulating the profile of the photoluminescence intensity with an interference visibility equal to 23%, the interference contrast possibly varying from  $\sim 12\%$  to 45% in our studies.

then to the ring shown in Fig. 2(b), making this interference pattern topologically recognizable.

Figure 2(c) shows an interference pattern measured in the same conditions as for the experiments of Fig. 1(b). Remarkably, this observation agrees quantitatively with the simulation for a condensate having one quantized vortex pinned at the center of the trap. This is shown in Figs. 2(d)–2(f) where the interference profiles taken at the center of the ring (e) and on its left and right, (d) and (f), respectively, are reproduced by modulating the photoluminescence intensity profile with 23% interference visibility. The contrast providing the fraction of bright excitons in the superfluid phase [33], we deduce that about one third of bright excitons evolve in a quantum condensed state for these experiments. Let us then stress that the results shown in Fig. 2(c) are obtained by postselecting a particular realization out of successive acquisitions, measured all under the same conditions. Such a postselection is necessary because our studies suffer from electrostatic fluctuations. In fact, it is only for a particular confinement landscape that an individual vortex is possibly revealed, as in Fig. 2(c). The electrostatic trapping potential has to be sufficiently regular for a superfluid to possibly form, and exhibit a defect capable to localize a single vortex around the center of trap, the position of this defect being stable all along the measurement time.

Without varying experimental conditions we also studied the evolution of quantum coherence while the exciton density varies in the trap. This is directly achieved by changing at the detection the delay to the end of the loading laser pulse [Fig. 1(a)]. To reach conclusions that are not limited by potential fluctuations during our measurements, we successively recorded a set of 20 interference patterns, every 10 ns after the loading pulse. Figure 3(a) shows that for delays shorter than 150 ns, i.e., when the trap confines more than about  $2 \times 10^4$  indirect excitons, interference fringes are not resolved in the photoluminescence. By contrast, from 150 to 200 ns after optical loading, i.e., when the population of excitons in the trap decreases from  $2 \times 10^4$  to  $10^4$ , Figs. 3(b), 3(c) show that bright excitons exhibit macroscopic spatial coherence: interference fringes are clearly resolved in patterns that cover the center of the trap, i.e., an approximately  $5 \times 5\ \mu\text{m}^2$  region. At longer delays ( $\gtrsim 200$  ns), however, interference fringes are not detected clearly in our experiments.

The absence of interference pattern when the trap confines less than about  $10^4$  excitons is not very surprising. Indeed, in this regime repulsive interactions between excitons yield a low mean-field energy, of the order of potential fluctuations ( $\sim 500\ \mu\text{eV}$  [20]). The trapped gas is then probably too dilute to establish long-range coherence by screening electrostatic disorder [34]. On the other hand, it is more surprising that quantum coherence is not observed beyond a maximum of about  $2 \times 10^4$  particles in the trap. Yet, this limit lies well in the dilute regime

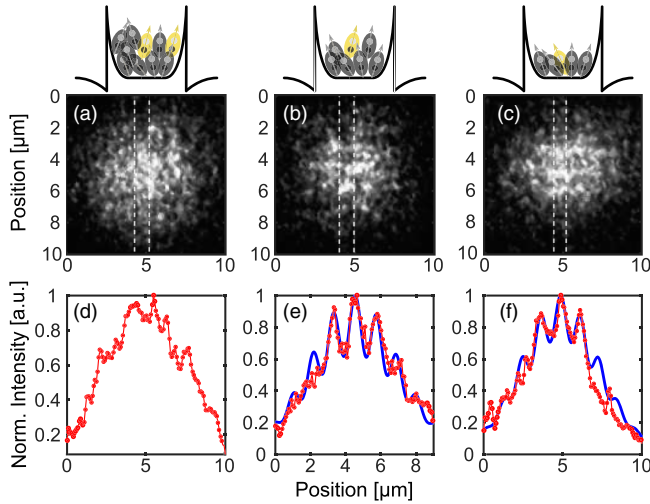


FIG. 3. (a)–(c) Interference patterns measured for a decreasing exciton density in the trap at  $T_b = 330$  mK, 120 (a), 150 (b), and 200 ns (c) after extinction of the loading laser pulse. We estimate that the total number of excitons is about  $4 \times 10^4$ ,  $2 \times 10^4$ , and  $10^4$ , respectively, the drawings on top illustrating the filling of the trap. The panels (d) to (f) show the corresponding interference profiles evaluated at the center of the trap (between the dashed lines). While in (d) our experiments do not reveal any interference, in (e) and (f) the interference visibility is 25% and 18%, respectively. Red points show experimental results and the blue lines the simulation obtained by modulating the intensity profile with the aforementioned visibilities.

which excludes the role of exciton ionization. However, excitons may already suffer from a too large deviation to ideal bosons beyond this range of density [35]. Also, one cannot exclude that beyond  $2 \times 10^4$  particles in the trap the strong dipolar interactions between excitons already lead to correlations which challenge the emergence of a collective quantum phase.

Last, we studied the dependence of the interference contrast as a function of the bath temperature. Let us restrict ourselves to the relevant range of delays to the loading laser pulse (150 to 200 ns). For the shortest delay, i.e., for  $\sim 2 \times 10^4$  indirect excitons in the trap, Fig. 4(a) shows that the photoluminescence exhibits long range order at the center of the trap, up to a critical temperature  $T_c \approx 1.3$  K. The interference visibility, i.e., the fraction of bright excitons contributing to the superfluid, follows well the theoretical scaling proportional to  $1 - (T_b/T_c)^2$  for two-dimensional particles in a trap [36]. Furthermore, Fig. 4(b) shows that  $T_c \sim 1$  K when the density is decreased by around twofold, i.e., at a delay of 200 ns after the loading pulse. This decrease of  $T_c$  is expected [36]; however, quantitative conclusions are difficult to raise since our experiments are limited by the weak photoluminescence intensity. As underlined in Fig. 4, our measurements suffer from a signal-to-noise ratio of less than 10, which leads to a minimum threshold for our interferometric detection of

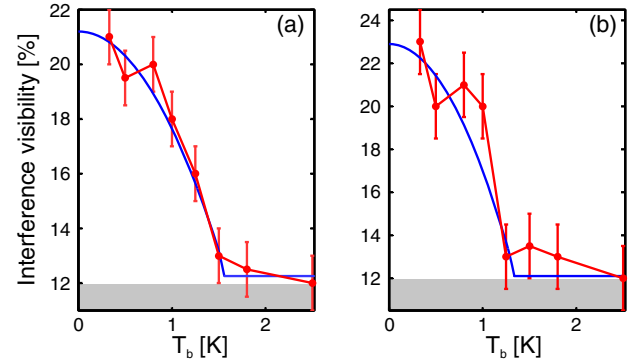


FIG. 4. Interference contrast measured at the center trap as a function of the bath temperature  $T_b$ . In (a) we show the visibilities measured in the regime where  $2 \times 10^4$  excitons occupy the trap, while the number of excitons is reduced to  $10^4$  for the measurements shown in (b). Solid blue lines show the theoretically expected  $1 - (T/T_c)^2$  scaling of the condensate fraction, with  $T_c \sim 1.3$  and 1 K for (a) and (b), respectively. In (a)–(b) the gray region marks the sensibility of our interferometric detection, i.e., the level fixed by the signal-to-noise ratio at the detection.

about 12%. Experiments displaying no evidence of spatial interference are then assigned 12% visibility.

Although quantum signatures are detected in the photoluminescence emitted by bright exciton states, crude estimations show that their occupation is too small to allow for a bright condensate independent from the underlying dominant population of optically dark excitons. Indeed, out of  $\sim 10^4$  excitons confined at  $T_b = 330$  mK, about 3/4 populate dark states [12]. By only considering the remaining fraction of bright excitons, the critical temperature for quantum degeneracy would be less than  $\sim 300$  mK [12]. A fragmented condensate of bright excitons would then contradict our experiments which, as shown in Fig. 4, reveal quantum coherence up to 1.3 K, as expected for a few  $10^4$  excitons in the trap. Considering limiting factors, such as the strength of electrostatic disorder, it is actually excluded that such a low density of bright indirect excitons possibly condenses alone [34]. This leads us to conclude that dark and bright states are coherently coupled in our experiments, leading to the theoretically predicted four-component superfluid of indirect excitons [4].

Finally, let us note that experiments with cold atomic gases have recently explored the superfluid quantum phase transition, by cooling a Bose gas at a variable rate. It was hence verified that the size of superfluid domains formed at the critical point decreases with the quenching rate [37,38], as prescribed by the Kibble-Zurek mechanism [39]. Here, we had to follow the opposite approach, because the bath temperature can be kept constant while the exciton density necessarily decreases slowly, due to radiative recombination. Thus, we observe that an initially dense gas, showing no evidence of long-range coherence, abruptly becomes superfluid below a critical density of a

few  $10^{10}$   $\text{cm}^{-2}$  at sub-Kelvin temperatures. In this regime, quantum signatures are resolved in the coherent photoluminescence radiated by the four-component and mostly dark condensate of excitons. Interestingly, this behavior is restricted for a narrow range of densities only.

The authors are grateful to Monique Combescot and Roland Combescot for their continuous support of this work and for many enlightening discussions. We would also like to thank Tristan Cren for stimulating discussions and Maciej Lewenstein for a critical reading of the manuscript. Our work has been financially supported by the projects INDEX (EU-FP7-ITN), XBEC (EU-FP7-CIG), and by OBELIX from the french Agency for Research (ANR-15-CE30-0020).

R. A. and M. B. contributed equally to this work.

\*Corresponding author.

francois\_dubin@icloud.com

- [1] A. J. Leggett, *Quantum Liquids* (Oxford University Press, New York, 2006).
- [2] *Bose-Einstein Condensation*, edited by L. P. Pitaevskii and S. Stringari (Oxford University Press, New York, 2003).
- [3] M. Combescot, O. Betbeder-Matibet, and R. Combescot, *Phys. Rev. Lett.* **99**, 176403 (2007).
- [4] R. Combescot and M. Combescot, *Phys. Rev. Lett.* **109**, 026401 (2012).
- [5] M. Combescot, R. Combescot, M. Alloing, and F. Dubin, *Phys. Rev. Lett.* **114**, 090401 (2015).
- [6] J. M. Blatt, K. W. Böer, and W. Brandt, *Phys. Rev.* **126**, 1691 (1962).
- [7] L. V. Keldysh and A. N. Kozlov, *Sov. Phys. JETP* **27**, 521 (1968).
- [8] R. Zimmerman, *Bose-Einstein Condensation of Excitons: Promise and Disappointment*, edited by A. L. Ivanov and S. G. Tikhodeev (Oxford University Press, New York, 2008).
- [9] M. Combescot, R. Combescot, and F. Dubin, *Rep. Prog. Phys.* (to be published).
- [10] M. Combescot and S. Y. Shiau, *Excitons and Cooper Pairs: Two Composite Bosons in Many-Body Physics* (Oxford Univ. Press, New York, 2016).
- [11] E. Blackwood, M. J. Snelling, R. T. Harley, S. R. Andrews, and C. T. B. Foxon, *Phys. Rev. B* **50**, 14246 (1994).
- [12] See Supplemental Material at <http://link.aps.org/supplemental/10.1103/PhysRevLett.118.127402> for experimental details and theoretical estimates.
- [13] L. V. Butov, *JETP* **122**, 434 (2016), and references therein.
- [14] D. Snoke, *Physica Status Solidi B* **238**, 389 (2003), and references therein.
- [15] A. V. Gorbunov and V. B. Timofeev, *J. Low Temp. Phys.* **42**, 340 (2016).
- [16] Y. E. Lozovik and V. I. Yudson, *Zh. Eksp. Teor. Fiz.* **71**, 738 (1976).
- [17] Y. E. Lozovik and O. L. Berman, *J. Exp. Theor. Phys.* **84**, 1027 (1997).
- [18] Y. Shilo, K. Cohen, B. Laikhtman, K. West, L. Pfeiffer, and R. Rapaport, *Nat. Commun.* **4**, 2335 (2013).
- [19] M. Alloing, M. Beian, M. Lewenstein, D. Fuster, Y. González, L. González, R. Combescot, M. Combescot, and F. Dubin, *Europhys. Lett.* **107**, 10012 (2014).
- [20] M. Beian *et al.*, [arXiv:1506.08020](https://arxiv.org/abs/1506.08020).
- [21] A. L. Ivanov, E. A. Muljarov, L. Mouchliadis, and R. Zimmermann, *Phys. Rev. Lett.* **104**, 179701 (2010).
- [22] C. Schindler and R. Zimmermann, *Phys. Rev. B* **78**, 045313 (2008).
- [23] A. V. Gorbunov and V. B. Timofeev, *JETP Lett.* **84**, 329 (2006).
- [24] A. A. High, A. K. Thomas, G. Grosso, M. Remeika, A. T. Hammack, A. D. Meyertholen, M. M. Fogler, L. V. Butov, M. Hanson, and A. C. Gossard, *Phys. Rev. Lett.* **103**, 087403 (2009).
- [25] M. Remeika, J. C. Graves, A. T. Hammack, A. D. Meyertholen, M. M. Fogler, L. V. Butov, M. Hanson, and A. C. Gossard, *Phys. Rev. Lett.* **102**, 186803 (2009).
- [26] G. Schinner, J. Repp, E. Schubert, A. K. Rai, D. Reuter, A. D. Wieck, A. O. Govorov, A. W. Holleitner, and J. P. Kotthaus, *Phys. Rev. Lett.* **110**, 127403 (2013).
- [27] K. Cohen, Y. Shilo, K. West, L. Pfeiffer, and R. Rapaport, *Nano Lett.* **16**, 3726 (2016).
- [28] M. Stern, V. Umansky, and I. Bar-Joseph, *Science* **343**, 55 (2014).
- [29] D. Nandi, A. D. K. Finck, J. P. Eisenstein, L. N. Pfeiffer, and K. W. West, *Nature (London)* **488**, 481 (2012).
- [30] X. Huang, W. Dietsche, M. Hauser, and K. von Klitzing, *Phys. Rev. Lett.* **109**, 156802 (2012).
- [31] A. F. Croxall, K. DasGupta, C. A. Nicoll, M. Thangaraj, H. E. Beere, I. Farrer, D. A. Ritchie, and M. Pepper, *Phys. Rev. Lett.* **101**, 246801 (2008).
- [32] J. A. Seamons, C. P. Morath, J. L. Reno, and M. P. Lilly, *Phys. Rev. Lett.* **102**, 026804 (2009).
- [33] M. Naraschewski and R. J. Glauber, *Phys. Rev. A* **59**, 4595 (1999).
- [34] O. L. Berman, Y. E. Lozovik, D. W. Snoke, and R. D. Coalson, *Phys. Rev. B* **70**, 235310 (2004).
- [35] M. Combescot and C. Tanguy, *Europhys. Lett.* **55**, 390 (2001).
- [36] I. Bloch, J. Dalibard, and W. Zwerger, *Rev. Mod. Phys.* **80**, 885 (2008).
- [37] C. N. Weiler, T. W. Neely, D. R. Scherer, A. S. Bradley, M. J. Davis, and B. P. Anderson, *Nature (London)* **455**, 948 (2008).
- [38] N. Navon, A. L. Gaunt, R. P. Smith, and Z. Hadzibabic, *Science* **347**, 167 (2015).
- [39] W. H. Zurek, *Phys. Rep.* **276**, 177 (1996).